A Stochastic Geometry Approach for the Analysis of Strip-Shaped Cooperative Multi-hop Wireless Networks

By

Asma Afzal

2011-NUST-MS-EE(S)-05

Supervisor

Dr. Syed Ali Hassan

Department of Electrical Engineering

A thesis submitted in partial fulfillment of the requirements for the degree of Masters in Electrical Engineering (MS EE-TCN)

In

School of Electrical Engineering and Computer Science,

National University of Sciences and Technology (NUST),

Islamabad, Pakistan.

(July 2013)

Approval

It is certified that the contents and form of the thesis entitled "**A Stochastic Geometry Approach for the Analysis of Strip-Shaped Cooperative Multi-hop Wireless Networks**" submitted by **Asma Afzal** have been found satisfactory for the requirement of the degree.

Advisor: **Dr. Syed Ali Hassan**

Signature: _____

Date: _____

Committee Member 1: **Dr. Adnan Khalid Kiani**

Signature: _____

Date: _____

Committee Member 2: **Dr. Khawar Khurshid**

Signature: _____

Date: _____

Committee Member 3: **Dr. Zawar Hussain Shah**

Signature: _____

Date: _____

Abstract

We consider a strip-shaped cooperative multi-hop wireless network stochastically model it with quasi-stationary Markov chain. The network is considered to be a fixed boundary decode-and-forward Opportunistic Large Array (OLA), where each level is of the same size and contains the same number of nodes placed randomly. The state of the system is represented by the number of nodes that decode the message in the current level. The distribution of the received power at a node is derived to formulate the transition probability matrix. For the distribution of power, a closed-form expression of the distribution of distance between a pair of nodes in disjoint levels is derived. It is seen that the distribution of distance can be well-approximated by the Weibull distribution. The Weibull approximation is then carried forward to find the distribution of the received power at a node assuming all nodes transmit with the same power and the channel has Rayleigh fading and path loss with an arbitrary exponent. The coverage and outage characteristics for various network sizes and path loss exponents are quantified. The signal-to-noise ratio (SNR) margin required for a given network coverage is determined by using the Perron-Frobenius theorem of non-negative matrices. Numerical simulations are performed to validate the theoretical results.

Certificate of Originality

I hereby declare that this submission is my own work and to the best of my knowledge it contains no materials previously published or written by another person, nor material which to a substantial extent has been accepted for the award of any degree or diploma at NUST SEECS or at any other educational institute, except where due acknowledgement has been made in the thesis. Any contribution made to the research by others, with whom I have worked at NUST SEECS or elsewhere, is explicitly acknowledged in the thesis.

I also declare that the intellectual content of this thesis is the product of my own work, except for the assistance from others in the project's design and conception or in style, presentation and linguistics which has been acknowledged.

Author Name: **Asma Afzal**

Signature: _____

To my parents.

Table of Contents

List of Figures

Chapter 1

Introduction

In wireless ad hoc networks, multi-hop communication is the most commonly used technique for long-range transmissions. A temporary path is formed from the point-to-point links through which the message can travel from the source to the destination. This reduces the transmit power and the overall cost of deployment, as the access point or base station does not need to directly communicate with each node in a centralized setup. However, wireless links are generally subject to multi-path fading and receiver thermal noise and the overall probability of successfully delivering a message from the source to the destination in multi-hop communication is the product of the probability of successful delivery at each link inside the path. Therefore, the overall probability of successful delivery is quite lower than an individual link probability of success. Packet retransmission at link layer is one of the solutions to make up for this loss of information, but this would consume extra power and will cause excessive delay. Cooperative transmission (CT) provides a solution to this problem as it exploits the inherent features of a wireless channel to improve link reliability and coverage range.

A fast and promising technique of CT at physical layer (PHY) is the Opportunistic Large Arrays (OLAs), whereby, the nodes which are arranged in an ad hoc manner, adopt the mechanism of controlled flooding to relay the message from the source to the destination or broadcast the message to the entire network. Nodes that receive a message and are able to successfully decode it, autonomously transmit it without the presence of any cluster-head or beacon node and this process continues in a multi-hop fashion. OLAs provide a low-power solution for long-distance wireless communication and are particularly suited for wireless sensor network (WSN) applications.

In this work, we stochastically model a strip-shaped decode-and-forward (DF) OLA network. To simplify our analysis, we divide the strip-shaped network into hypothetical contiguous square regions, containing nodes placed randomly and the transmissions from nodes in one level are considered to be confined to the boundaries of the adjacent levels only. This stochastic design will act as a prelude to finding the coverage aspects of random boundary cooperative ad hoc networks and for more general strip networks. We assume that all nodes transmit the same power and that correct decoding occurs if the aggregate received power at a node exceeds a certain modulation-dependent decoding threshold. The MAC layer issues involving orthogonal channel assignment and interference mitigation have not been addressed. We assume that the transmissions take place over interference-free orthogonal fading channels. We model our transmissions with a well-known quasi-stationary Markov chain [2] based on the assumption that the transmissions travel enough hops to reach a steady state and the conditional probability that a node successfully decodes in a certain level given that at least

one node transmitted in the previous level is same for each level in the strip network. Once the system attains the quasi-stationary state distribution, useful performance metrics such as the end-to-end success probability, coverage range, network size and the required transmit power can be computed. Our main contributions are:

- An exact distribution of the Euclidean distance between two nodes randomly placed in non-overlapping contiguous square regions is derived.
- With a moment matching approach, we show that distance raised to any positive power is Weibull distributed.
- We find the distribution of the single-input single-output (SISO) power at a node, which is the ratio of a unit-mean exponential random variable (RV) and a Weibull RV. This result is also not explicitly stated in the relevant literature.
- We find the distribution of the sum of N such independent and identically distributed (I.I.D) ratio RVs, which is the distribution of received power for a virtual multiple-input single-output (MISO) network.
- We finally show how the network in consideration can be modeled with the help of a quasi-stationary Markov chain.

Chapter 2

Background and Literature Review

2.1 Modeling Cooperative Networks

A lot of research has been done on techniques involving cooperative communication in the past few years. In wireless networks, CT gains much attention as it helps enhancing the system performance by providing diversity gains. In CT, multiple devices transmit the same message to the destination using uncorrelated fading channels. This improves the overall link reliability and provides range extension. Conventional cooperative systems made use of a single relay, which would transmit the same message as the source to the destination [3], [4]. As we can see in Fig. 2.1, node S has to communicate wirelessly with node D. The top-most line in Fig. 2.1 represents the outage probability for various values of signal-to-noise ratio (SNR) [4]. Node D is considered to go into outage if the power received by node D drops below a certain threshold of SNR. However, with the help of a relay node,

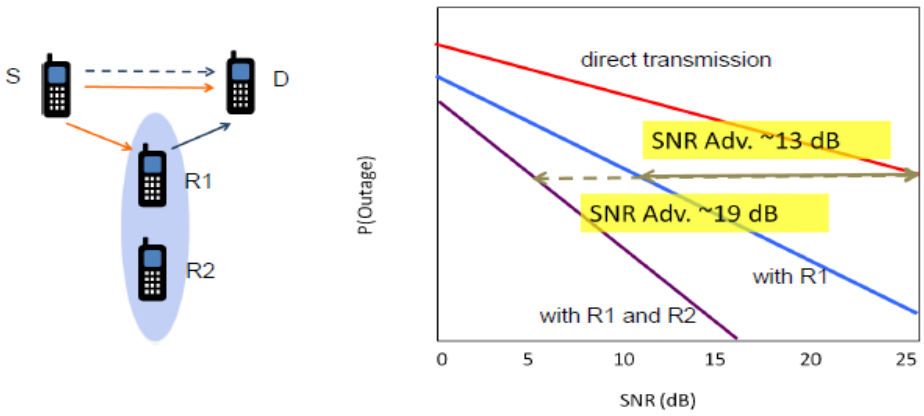

Figure 2.1: (Left): Cooperative and direct transmission topologies. (Right): Probability of outage for a given SNR for these topologies. [1]

R1, the outage probability significantly drops down as it can be observed by the middle line in Fig. 2.1. The advantage of SNR is approximately 13 dBs, which means that in case where S is transmitting alone, an additional 13 dBs of power has to be transmitted to maintain the same outage probability as when S-R1 pair is transmitting. Adding another relay node R2, provides an additional SNR advantage of 3dBs. Therefore, CT improves the reliability of a system.

The two most commonly used relaying techniques in cooperative transmission involve amplify-and-forward (AF) transmission and decode-and-forward (DF) transmission. In the former technique, the relay node amplifies the arriving signal and transmits it while in the latter technique, the relay node decodes the arriving signal, re-encodes and then transmits it [4]. Correct decoding takes place if the SNR of the received signal is above a certain decoding threshold. Several methods have been proposed for SNR-estimation for different modulation techniques [5–7].

A lot of research has been done on cooperative networks having a single relay node. While some authors have focused on the outage behaviors and channel capacity of a network [8], [9], others have proposed ways to design a receiver such the the effect of inter-symbol interference (ISI) and the bit error rate (BER) in transmission is minimized [10]. Researchers have also considered dual relay schemes [11] or approaches with multiple relays in which a group of relay nodes help the source in successfully delivering data to the destination and range extension [12, 13]. Optimization in such designs can be in terms of selecting the most appropriate relay (which is closer to the destination etc.) as discussed in [14] and [15]. A multiple relay techniques proposed in [16] incorporates feedback as well. These techniques show that cooperative communication finds its use in a number of applications of the wireless networks.

Cooperative networks like Opportunistic Large Arrays (OLAs) [17], are well-suited for multi-hop communication where a group of nodes transmits the same message to another group of nodes. This process continues in a multi-hop manner. Owing to the simplicity in their implementation, OLAs have gained immense popularity [18–31]. OLAs provide a low-power solution for long-distance wireless communication and are particularly suited for wireless sensor network (WSN) applications. In an OLA network, when the source node sends a message in the first time slot, nodes within its range receive the message. Nodes which are able to successfully decode the message, become a part of level 2 nodes as they retransmit the same message in the second time slot. This process continues until the message reaches the destinations.

One of the techniques proposed to model OLAs shows that if the node density approaches infinity for a fixed power per unit area and the decoding threshold is below is a certain critical value, successful decoding is guaranteed no matter how far is the destination [32]. Because of the assumption of a *continuum* of nodes, this model is only applicable on dense wireless networks. The authors in [33] consider a finite density grid-based linear OLA and model their network with a quasi-stationary Markov chain. Their analytical results prove that infinite propagation is not guaranteed in case of finite density OLAs, but the success probability or reaching a particular distance can be calculated with the help of the developed model. This model is extended in [34] for linear networks with nodes placed according to a Bernoulli point process and it shown in [35] that co-locating a group of nodes in these linear networks provides a fixed SNR advantage.

For 2-dimensional finite density ad hoc networks, extension of the model in [34] is not quite straight-forward. This is because the candidate locations for nodes are not known and a node could be present any where in a given area. Many cooperative approaches, specifically for strip-shaped networks, also require that the cooperating nodes of two adjacent levels form disjoint sets [33, 36, 37].

2.2 Distribution of the Euclidean Distance

As the locations of nodes are random in this study, path loss is no longer deterministic and depends on the Euclidean distance between the nodes. In [38], a comprehensive survey is done on the distribution of distances between nodes for two main network topologies. The first is when the nodes are spread

according to a Poisson Point Process (PPP) on a place and the second is when the nodes are independent and uniformly distributed (IUD) over some region of plane which is either a circle or a rectangle. Some applications require the distribution of distances between a node and its nearest neighbor [39] to check connectivity of a network. In [40], the author derives the distribution of Euclidean distance between two nodes present in a rectangular region.

We extend the work of [40] and derive the distribution of Euclidean distance for nodes placed in disjoint but contiguous square regions, which, to the best of our knowledge, does not exist in the relevant literature.

Chapter 3

Network Description

In this chapter, we describe the network topology and state the assumptions used for computation of the received power. Consider a strip-shaped extended network where the size of the network grows in the horizontal dimension for a fixed node density as shown in Fig. 3.1. Let ϕ denote a binomial point process on a compact set $\mathcal{A} \in \mathbb{R}^2$ such that $\mathcal{A}$ is a bounded LxL square region. A total of N points are uniformly distributed in the bounded set $\mathcal{A}$, where $\phi(\mathcal{A}) = N$ with probability 1. Multiple such point processes form a fixed-boundary strip-shaped network, where the boundaries of each level are pre-defined and occur at regular intervals of size L. Each level consists of a fixed number, N, of nodes placed randomly. This scenario can be attributed to a hallway consisting of adjacent rooms of equal sizes where sensor nodes are placed randomly in each room for monitoring purposes. In this type of cooperative network, the nodes at level $n-1$ transmit the same message and all the nodes in level n try to decode it. The nodes which are able to decode the message successfully become part of level n decode-and-forward (DF) nodes and this process continues. It is assumed that the transmissions

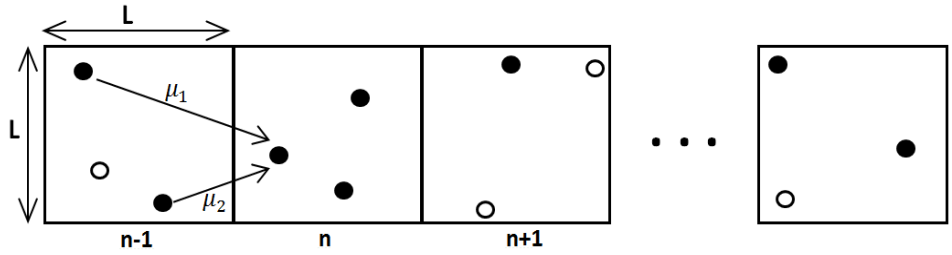

Figure 3.1: A realization of a fixed boundary strip network with randomly placed nodes.

from one level of nodes occur synchronously over orthogonal fading channels and every node has the same transmit power, P_t. Nodes at level n make use of diversity combining to decode the message arriving from level $n-1$ only. If the aggregated received SNR through superimposition is above a certain modulation-defined threshold, τ, the message is assumed to be correctly decoded and will be immediately transmitted in the next time slot. A hop occurs, if at least one node in the next level is able to decode the message. This fixed boundary network is opportunistic in the sense that a node at a level n may or may not be able to decode the message arriving from level $n-1$. For example, in Fig. 3.1, the filled circles represent the DF nodes whereas the hollow circles represent the nodes that have not decoded the message. Correct decoding depends on the channel conditions and the location of the node itself; both of which are random. We consider two independent channel impairments; path loss, where signal attenuates non-linearly with respect to the increase in distance and Rayleigh fading. If Q_{n-1} denotes the set of DF nodes at level $n-1$ with cardinality $|Q_{n-1}|$, where $\sup_n |Q_n| \leq N$, the expression for received power, P_r, by a node i at level n from the previous level

nodes is given as,

$$P_{r_i}(n) = \sum_{j \in Q_{n-1}} \frac{P_t \mu_{ij}}{d_{ij}^{\alpha}}, \tag{3.1}$$

where $d_{ij} \in \mathbb{R}^2$ is the Euclidean distance between nodes i and j, μ_{ij} characterizes a unit-mean exponential random variable (RV), which is the squared envelope of the signal undergoing Rayleigh fading and α denotes the path loss exponent. It can be noticed that (3.1) describes the received power for a multi-path multiple-input single-output (MISO) system and the transmissions propagate as a virtual MISO.

Throughout this document, we use the following notations: upper case alphabets represent RVs and lower case alphabets are their respective realizations. '$F_X(x)$' denotes the cumulative distribution function (CDF) of RV X while '$f_X(x)$' denotes its probability density function (PDF).

Chapter 4

Modeling by Markov Chain

In this chapter, we model the transmissions that propagate from one level to another under the impacts of wireless channel.

4.1 State Definition

As discussed previously, a randomly selected node at level n receives multiple copies of the same message signal and correct decoding is assumed if the received power is above a threshold after post-detection combining. Thus, the state of a node i at level n can be described by a binary random variable, $\mathbb{I}_i(n)$, such that

$$\mathbb{I}_i(n) = \begin{cases} 1 & \text{if } P_{r_i}(n) \geq \tau, \\ 0 & \text{if } P_{r_i}(n) < \tau. \end{cases} \tag{4.1}$$

The combination of the individual node states, $[\mathbb{I}_1(n)\mathbb{I}_2(n)...\mathbb{I}_N(n)]$, is a binary N tuple representing the overall state of the system at level n. For instance, when $N = 3$, [100] signifies that a single node has decoded the

message out of a total of three nodes. If the nodes are placed deterministically, the combinations $[010], [100]$ and $[010]$ can be treated as separate states. This is because the distance between node i in the current level and node j in the previous level is distinct and fixed. However, when the nodes' locations are random, different permutations of a state are effectively the same as the inter-nodal distance is also random. We say that a level is in state **1** if any one of the nodes is able to decode the message while the rest of the nodes have failed to decode. Therefore, the state of the system at instant n can be defined as the number of DF nodes at that level. Specifically, if $\mathcal{B}(n)$ defines the state of the system at level n, then

$$\mathcal{B}(n) = \sum_{i=1}^{N} \mathbb{I}_i(n). \tag{4.2}$$

It can be further noticed that the state of the system at time n depends only upon the previous state, making $\mathcal{B}$ a finite-state Markov process. The assumptions that the transmissions take place at discrete-time instants and the channel statistics remains the same over the entire network result in a homogenous discrete-time Markov chain, $\mathcal{B}$. The Markov chain, $\mathcal{B}$, is defined on two mutually exclusive sets, i.e., $\mathcal{B} \in \{0\} \text{ U } \mathbf{S}$, where $\mathbf{S}$ is the transient state space given as

$$\mathbf{S} = \begin{cases} \mathbf{1} & \text{Exactly one node decodes,} \\ \mathbf{2} & \text{Exactly two nodes decode,} \\ . & \\ . & \\ \mathbf{N} & \text{All nodes decode,} \end{cases} \tag{4.3}$$

and **0** is the absorbing state. The absorbing state refers to the state of the system when no node can decode the message and the transmissions stop propagating. On the other hand, the states in **S** make an irreducible state space with cardinality $|\mathbf{S}| \leq N$. Hence, the Markov chain can be characterized by defining an $(N+1) \times (N+1)$ transition probability matrix, $\mathbf{H}$, which is a right stochastic matrix containing transition probabilities for all possible states. As the Markov chain will eventually be absorbed, i.e., $\lim_{n\to\infty} \mathbb{P}\{\mathcal{B}(n) = 0\} \to 1$, it is desired to find the state of the system just before absorbing occurs. This conditional state distribution is known as the quasi-stationary distribution and is defined by invoking the Perron-Frobenius (PF) theorem of non-negative matrices. Therefore, we remove the row and column corresponding to the absorbing state (state **0**) of $\mathbf{H}$ to get a sub-matrix $\tilde{\mathbf{H}}$ with active state transition probabilities only. According to the PF theorem [41], a unique maximum eigenvalue, ρ, and its unique corresponding left eigenvector, $\hat{\mathbf{v}}$, exists for $\tilde{\mathbf{H}}$ such that this eigenvector gives the quasi-stationary distribution of the Markov chain under consideration. In our case, $\tilde{\mathbf{H}}$ is an irreducible $N \times N$ square matrix with positive entries. Furthermore, $\tilde{\mathbf{H}}$, is not right stochastic as the row probabilities no longer sum to one, which implies that

$$0 < \rho < 1. \tag{4.4}$$

The conditional probability of being in a state s is given as

$$\mathbb{P}\{\mathcal{B}(n) = s | T_k > n\} = v_s, \quad s \in \mathbf{S}, \tag{4.5}$$

where v_s is the sth entry of the normalized eigenvector $\mathbf{v} = \hat{\mathbf{v}}/\sum_s \hat{\mathbf{v}}_s$ and T_k is the killing time defined as

$$T_k = \inf\{n \geq 0; \mathcal{B}(n) = 0\}. \tag{4.6}$$

Thus, the propagation modeling in this opportunistic network boils down to finding the transition probability matrix for the active states only. We will derive this matrix for single-input single-output (SISO) and multiple-input single-output (MISO) networks in the subsequent sections.

4.2 Formulating the State Transition Matrix

To compute the state transition probabilities in $\tilde{\mathbf{H}}$, we need to find the success/outage probability of each node in a certain level, n, given that $|Q_{n-1}|$ nodes transmitted in the previous level. It is important to note that if $|Q_{n-1}|$ and other network parameters (e.g. region length, L, path loss exponent, α and transmit power, P_t) are kept constant, the success/outage probability for all N nodes in a particular level n will be the same. This is because the received power in (3.1) is a doubly stochastic RV where the distance between the nodes and the fading gains are both random. The success probability, P_s, of a node i at level n, defined as the probability of successfully decoding the message is expressed as

$$\begin{aligned} P_s &= \mathbb{P}\{\mathbb{I}_i(n) = 1 | \mathcal{B}(n-1) \in \mathbf{S}\} \\ &= \mathbb{P}\{P_{r_i}(n) \geq \tau | \mathcal{B}(n-1) \in \mathbf{S}\} \quad \forall i = \{1, 2, ..., N\}. \end{aligned} \tag{4.7}$$

The conditional probability that the Markov chain will be in state s_2 given that the system was in state s_1 in the previous level; $(s_1, s_2 \in \mathbf{S})$, can be

calculated by applying the binomial theorem such that

$$\begin{aligned}\mathbb{P}(s_2|s_1) &= \binom{N}{s_2} P_s^{s_2}(1-P_s)^{N-s_2}, \\ &= \binom{N}{s_2} P_s^{s_2}(P_o)^{N-s_2},\end{aligned} \tag{4.8}$$

where $P_o = 1 - P_s$ is the outage probability of a node. Also, it can be noticed from (4.7) that the success probability of the i^{th} node is given as

$$P_s = \int_{\tau}^{\infty} f_{P_{r_i|s_1}}(t)dt, \tag{4.9}$$

where $f_{P_{r_i|s_1}}(t)$ is the conditional distribution of the received power in (3.1).

4.2.1 Derivation of the Distribution of Euclidean Distance

We begin the derivation of the distribution of received power at a node by first finding the distribution of the Euclidean distance between two nodes randomly placed in disjoint levels. Then we derive the distribution of the ratio between a unit-mean exponential RV and the distance RV raised to an arbitrary power α. We notice that this ratio distribution is essentially the distribution of power in case of SISO networks where there is a single sender in the previous level. For a typical MISO case, we derive the distribution of power by finding the distribution of the sum of the ratios of aforementioned RVs.

Lemma 1. *The distribution of the squared Euclidean distance, Z, between a pair of nodes randomly placed in disjoint contiguous $L \times L$ square regions is*

given as

$$f_Z(z) = \begin{cases} 0 & z \leq 0, z > 5L^2, \\ \frac{\sqrt{z}}{L^3} - \frac{z}{2L^4} & 0 < z \leq L^2, \\ \frac{1}{L^2}\left[\frac{3}{2} + \pi - 2sin^{-1}\sqrt{\frac{L^2}{z}}\right] & \\ -\frac{2}{L^3}\left[\sqrt{z} + \sqrt{z - L^2}\right] + \frac{z}{L^4} & L^2 < z \leq 2L^2, \\ \frac{1}{L^2}\left[2sin^{-1}\sqrt{\frac{L^2}{z}} - \frac{1}{2}\right] & \\ -\frac{2}{L^3}\left[\sqrt{z} - \sqrt{z - L^2}\right] & 2L^2 < z \leq 4L^2, \\ \frac{1}{L^2}\left[-\frac{5}{2} + 2tan^{-1}\sqrt{\frac{4L^2}{z-4L^2}}\right. & \\ \left. -2tan^{-1}\sqrt{\frac{z-L^2}{L^2}}\right] - \frac{z}{2L^4} + & \\ \frac{1}{L^3}\left[2\sqrt{z - L^2} + \sqrt{z - 4L^2}\right] & 4L^2 < z \leq 5L^2. \end{cases} \tag{4.10}$$

Proof. Let (x_1, y_1) and $(x_2 + L, y_2)$ represent two random points in disjoint square regions $\mathcal{A}_1$ and $\mathcal{A}_2$, respectively as shown in Fig. 4.1. The Euclidean distance between the two points is given as

$$d = \sqrt{((x_2 + L) - x_1)^2 + (y_2 - y_1)^2}, \tag{4.11}$$

where $x_i \in X_i$ and $y_i \in Y_i \ \forall \ i \in \{1, 2\}$. Random variables X_i and Y_i are independent and uniformly distributed (IUD) over $[0, L]$ such that $\forall i = \{1, 2\}$,

$$f_{X_i}(x) = f_{Y_i}(x) = \begin{cases} \frac{1}{L} & 0 < x < L \\ 0 & \text{elsewhere.} \end{cases} \tag{4.12}$$

Let $\Delta_X \doteq X_2 + L - X_1$. As X_1 and X_2 are both IUD RVs, the distribution of Δ_X is obtained using a convolution integral

$$f_{\Delta_X}(\Delta_X) = \int_{-\infty}^{\infty} f_{X_1=x}(x - \Delta_X) f_{X_2=x}(x - L) dx, \tag{4.13}$$

Solving the integral we get,

$$f_{\Delta_X}(\Delta_x) = \begin{cases} 0 & \Delta_x \leq 0, \Delta_x > 2L, \\ \frac{\Delta_x}{L^2} & 0 < \Delta_x \leq L, \\ \frac{1}{L^2}\left[2L - \Delta_x\right] & L < \Delta_x \leq 2L. \end{cases} \tag{4.14}$$

The expression for the PDF, $f_{\Delta_Y}(\Delta_y)$, of $\Delta_Y \doteq Y_2 - Y_1$ is given as

$$f_{\Delta_Y}(\Delta_y) = \begin{cases} 0 & \Delta_y \leq -L, \Delta_y > L, \\ \frac{1}{L^2}\left[L + \Delta_y\right] & -L < \Delta_y \leq 0, \\ \frac{1}{L^2}\left[L - \Delta_y\right] & 0 < \Delta_y \leq L. \end{cases} \tag{4.15}$$

For the next step, we find the PDF, $f_{\Delta_X^2}(x)$, which is non-zero for $0 \leq x \leq 4L^2$ and is zero elsewhere. Using Theorem 13.2 of [42], a simple derivation yields

$$f_{\Delta_X^2}(x) = \begin{cases} 0 & x \leq 0, x > 4L^2, \\ \frac{1}{L^2} & 0 < x \leq L^2, \\ \frac{1}{L\sqrt{x}} - \frac{1}{2L^2} & L^2 < x \leq 4L^2. \end{cases} \tag{4.16}$$

Again, we see that because of no offset in the y coordinates, the PDF, $f_{\Delta_Y^2}(y)$, is given as

$$f_{\Delta_Y^2}(y) = \begin{cases} 0 & y \leq 0, y > L^2, \\ \frac{1}{L\sqrt{y}} - \frac{1}{L^2} & 0 < y \leq L^2. \end{cases} \tag{4.17}$$

It is obvious that the distributions of Δ_X^2 and Δ_Y^2 are not identical. Now, for the expression of the PDF of the squared Euclidean distance, we need to find

the distribution, $f_Z(z)$, of $Z = \Delta_X^2 + \Delta_Y^2$, where $d^2 \in Z$. Since Δ_X^2 and Δ_Y^2 are independent, $f_Z(z)$ can again be represented as a convolution integral as

$$f_Z(z) = \int f_{\Delta_X^2}(u) f_{\Delta_Y^2}(z-u) \quad du. \tag{4.18}$$

Solving the integral, we get the piece-wise continuous PDF of the squared distance in (4.10). □

From Lemma 1, we see that the squared distance, $d^2 \in Z$, between two nodes in disjoint levels is distributed between 0 and $5L^2$. The offset of L can be applied in y-axis instead of x-axis without the loss of generality to obtain the same distribution of the squared distance for a vertically extended strip network. We move on to finding the distribution of distance raised to a positive power, α.

Corollary 1. *For the network in Fig. 4.1, the distribution of the Euclidean distance raised to an arbitrary power, α, where $d^\alpha \in \nu$ and $\nu = Z^{\frac{\alpha}{2}}$ is*

$$f_\nu(\nu) = \frac{2}{\alpha} \nu^{\frac{2}{\alpha}-1} f_Z(\nu^{\frac{2}{\alpha}}). \tag{4.19}$$

Even though an exact closed-form expression for the PDF of $d^\alpha \in \nu$ in (4.19) is obtained, it contains several non-linear terms that make further analysis difficult and unmanageable. As the PDF in (4.10) is smooth and satisfies all the conditions of regularity [43], it can be approximated with a simpler function, which encapsulates all features of the expression given in (4.10) as shown in the following Lemma.

Lemma 2. *For the network shown in Fig. 4.1, the distribution of the squared Euclidean distance, Z, between a pair of nodes can be approximated by Weibull distribution with a constant shape parameter, $k = 1.5806$, and a variable scale parameter, $\lambda = 4L^2/(3\Gamma(1.6327))$.*

Proof. We match the first two moments of a Weibull RV with the moments of Z to show that the Weibull distribution closely matches the exact distribution. The expected value of the squared distance is calculated as

$$\mathbb{E}[Z] = \int_0^{5L^2} z f_Z(z) dz = \frac{4}{3} L^2, \tag{4.20}$$

where $\mathbb{E}[.]$ denotes the expectation operator. Similarly, the second moment of the squared distance is given as

$$\mathbb{E}\left[Z^2\right] = \int_0^{5L^2} z^2 f_Z(z) dz = \frac{227}{90} L^4. \tag{4.21}$$

Weibull distribution is characterized by its shape and scale parameter (k and λ, respectively). A Weibull distributed RV, W, has mean

$$\mathbb{E}[W] = \lambda \Gamma(1 + \frac{1}{k}), \tag{4.22}$$

and variance

$$Var[W] = \lambda^2 \Gamma(1 + \frac{2}{k}) - \mathbb{E}[W]^2, \tag{4.23}$$

where $\Gamma(x)$ is the complete Gamma function. As $\mathbb{E}[W^2] = Var[W] + \mathbb{E}[W]^2$, we get the second moment of W, which is

$$\mathbb{E}[W^2] = \lambda^2 \Gamma(1 + \frac{2}{k}). \tag{4.24}$$

We apply the moment matching approach and solve the following set of non-linear equations to obtain the values of Weibull parameters in terms of the region size, L.

$$\begin{aligned} \lambda \Gamma(1 + \frac{1}{k}) &= \frac{4}{3} L^2, \\ \lambda^2 \Gamma(1 + \frac{2}{k}) &= \frac{227}{90} L^4. \end{aligned} \tag{4.25}$$

After eliminating λ in (4.25), the equation is solved numerically for k. We get a constant value of $k = 1.5806$. The value of λ is then calculated to be $4L^2/(3\Gamma(1.6327))$. We will show in Section 5 that the Weibull distribution with the calculated parameters closely matches the actual distribution of squared distance in (4.10). Hence, the new distribution of squared distance is given as

$$f_Z(z) \approxeq \frac{k}{\lambda^k} z^{k-1} e^{-(\frac{z}{\lambda})^k} \qquad z > 0. \tag{4.26}$$

□

Corollary 2. *Using Lemma 2 and Corollary 1 , the distribution of the Euclidean distance raised to any positive power, α, is also Weibull distributed and is given as*

$$f_\nu(\nu) \approxeq \frac{c}{\chi^c} \nu^{c-1} e^{-(\frac{\nu}{\chi})^c} \qquad \nu > 0. \tag{4.27}$$

where, $c = 2k/\alpha$ and $\chi = \lambda^{\alpha/2}$.

Here we notice that the addition of a path loss exponent simply alters the shape and scale parameters of the Weibull distribution in (4.26).

4.2.2 Received power for SISO networks: Distribution of the Ratio of Exponential and Weibull Random Variable

The next step is to find the distribution of the ratio of two RVs namely μ and ν (SISO case) and the sum of ratios (MISO case). The former case is derived in the following Lemma.

Lemma 3. *The ratio, R, of an exponential RV, $\mu \sim exp(1)$, and a Weibull RV, $\nu \sim Wbl(c, \chi)$, has the following distribution.*

for $c \geq 1$ ($\alpha \leq 3.1612$),

$$f_R(r) = \chi \sum_{n=0}^{\infty} \frac{1}{n!} \Gamma\left(\frac{1+c+n}{c}\right) (-r\chi)^n . \tag{4.28a}$$

and for $c < 1$ ($\alpha > 3.1612$),

$$f_R(r) = c\,(\chi)^{-c} \sum_{n=0}^{\infty} \frac{\Gamma(1+c+cn)}{n!} \left(-\frac{1}{\chi^c}\right)^n (r)^{-cn-c-1} , \tag{4.28b}$$

Proof. In [44], the authors have derived a closed-form expression for the distribution of the ratio of Gamma and Weibull RVs. The PDF of a Gamma random variable, G is

$$f_G(g) = \frac{\theta^\gamma}{\Gamma(\gamma)} g^{\gamma-1} e^{-g\theta} \qquad g > 0. \tag{4.29}$$

where γ and θ are the shape and scale parameters, respectively. We note that when γ and θ are fixed to 1, the Gamma distribution simplifies to

$$f_G(g) = e^{-g}, \quad \gamma = \theta = 1, \;\; g > 0, \tag{4.30}$$

which is essentially the PDF of a unit-mean exponential RV. Hence, $\mu \equiv G$. The corresponding CDF given as

$$F_G(\mu) = F_\mu(\mu) = 1 - e^{-\mu}, \quad \gamma = \theta = 1, \;\; \mu > 0. \tag{4.31}$$

Using (4.27) and (4.31), the CDF of $R = \mu/\nu$ is given as

$$\begin{aligned} F_R(r) &= \int_0^\infty F_\mu(r\nu) f_\nu(\nu) d\nu \\ &= 1 - \frac{c}{\chi^c} \int_0^\infty e^{-r\nu} \nu^{c-1} e^{-(\frac{\nu}{\chi})^c} d\nu, \end{aligned} \tag{4.32}$$

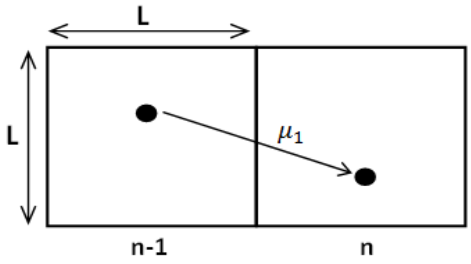

Figure 4.1: A realization of SISO network with randomly placed nodes in adjacent levels.

where $\Gamma(x, y)$ is the incomplete Gamma function. The integral in (4.32) is calculated using Equation (2.10.1.5) of [45] and is simplified as

for $c \geq 1$ ($\alpha \leq 3.1612$),

$$F_R(r) = r\chi \sum_{n=0}^{\infty} \frac{1}{(n+1)!} \Gamma\left(\frac{1+c+n}{c}\right) (-r\chi)^n . \tag{4.33a}$$

and for $c < 1$ ($\alpha > 3.1612$),

$$F_R(r) = -(r\chi)^{-c} \sum_{n=0}^{\infty} \frac{\Gamma(1+c+cn)}{(n+1)!} \left(-\frac{1}{r^c \chi^c}\right)^n , \tag{4.33b}$$

A simple differentiation operation results in the ratio PDF, $f_R(r) = \frac{dF_R(r)}{dr}$ in (4.28). □

After deriving the PDF of the ratio of RVs, we now derive the outage probability of SISO network in Fig. 4.1. Specifically, the outage probability of ith node in level n ($i \equiv 1$ in SISO) is given as $\mathbb{P}\{P_{r_i}(n) < \tau\}$, where $P_{r_i}(n) = P_t\mu/\nu$. We consider the following theorem.

Theorem 1 (**Outage Probability of SISO Network**). *If two nodes are randomly placed in contiguous $L \times L$ square regions as shown in Fig. 4.1 and*

a node transmits to another node in the presence of Rayleigh fading and path loss with an arbitrary exponent, then the outage probability, $P_o^{(SISO)}$, is given as

for $c \geq 1$,

$$P_o^{(SISO)} = \frac{\tau\chi}{P_t} \sum_{n=0}^{\infty} \frac{1}{(n+1)!} \Gamma\left(\frac{1+c+n}{c}\right) \left(-\frac{\tau\chi}{P_t}\right)^n. \tag{4.34a}$$

and for $c < 1$,

$$P_o^{(SISO)} = -\left(\frac{\tau\chi}{P_t}\right)^{-c} \sum_{n=0}^{\infty} \frac{\Gamma(1+c+cn)}{(n+1)!} \left(-\frac{P_t^c}{\tau^c\chi^c}\right)^n, \tag{4.34b}$$

Proof. Using Lemma 3 and the scaling property of RV ($\mathbb{P}\{aX < x\} = \mathbb{P}\{X < x/a\}$), we obtain the outage probability in (4.34). □

4.2.3 Received power for virtual MISO networks: Distribution of the sum of Ratio Random Variables

Now we focus our attention to the virtual MISO network of Fig. 3.1. To determine the outage probability in this case, the CDF of the received power in (3.1) needs to be calculated. Expanding (3.1), we have

$$\begin{aligned} P_{r_i}(n) &= P_t \left[\frac{\mu_1}{\nu_1} + \frac{\mu_2}{\nu_2} + ...\frac{\mu_\sigma}{\nu_\sigma}\right] \\ &= P_t[R_1 + R_2 + ... + R_\sigma] \quad \sigma = |Q_{n-1}|. \end{aligned} \tag{4.35}$$

As the RVs, $[R_1, R_2..., R_\sigma]$, are independent and identically distributed (IID), the PDF of the received power is σ-times self-convolution of $f_R(r)$ in (4.28). The additional parameter of transmit power, P_t simply scales the resulting distribution. The generalization of the final distribution, however, is highly

prohibitive with multiple self convolutions of $f_R(r)$. Hence, we proceed with carrying out our analysis in the Laplace domain.

Theorem 2 (**Outage Probability of MISO Network**). *The outage probability, P_o for an arbitrary node at level n in the virtual MISO network of Fig. 3.1 with pathloss exponent, $\alpha \leq 3.1612$, is given by*

(4.36)
$$P_o = \chi^{\sigma} \sum_{a_1=0}^{\infty} ... \sum_{a_\sigma=0}^{\infty} \frac{(\tau/P_t)^{a_1+a_2+...+a_\sigma+\sigma}}{(a_1+a_2+...+a_\sigma+\sigma)!} \prod_{i=1}^{\sigma} \Gamma\left(\frac{1+c+a_i}{c}\right) (-\chi)^{a_i},$$

Proof. As $\frac{r^n}{n!} \overset{\mathcal{L}}{\rightarrow} \frac{1}{s^{n+1}}$, the Laplace transform, $\mathcal{F}(s)$, of $f_R(r)$ in (4.28a) is given as

$$\mathcal{F}(s) = \chi \sum_{n=0}^{\infty} \Gamma\left(\frac{1+c+n}{c}\right) (-\chi)^n \frac{1}{s^{n+1}}. \tag{4.37}$$

Moreover, since the RVs $\{R_k\}_{k=1}^{\sigma}$ are IID, the Laplace transform of the PDF of their sums is written as

$$\mathcal{L}\left[\overset{\sigma}{\underset{k=1}{*}} f_{R_k}(r_k)\right] = \prod_{k=1}^{\sigma} \mathcal{F}_k(s) = [\mathcal{F}(s)]^{\sigma}, \tag{4.38}$$

where $*_{k=1}^{\sigma}$ denotes the self-convolutions of PDFs. When $\mathcal{F}(s)$ is raised to a power $\sigma = |Q_{n-1}|$, which is the number of transmitters in the previous level, we get

$$\begin{aligned} [\mathcal{F}(s)]^{\sigma} &= \left[\chi \sum_{n=0}^{\infty} \Gamma\left(\frac{1+c+n}{c}\right) (-\chi)^n \frac{1}{s^{n+1}}\right]^{\sigma} \\ &= \chi^{\sigma} \sum_{a_1=0}^{\infty} ... \sum_{a_\sigma=0}^{\infty} \prod_{i=1}^{\sigma} \Gamma\left(\frac{1+c+a_i}{c}\right) (-\chi)^{a_i} \frac{1}{s^{a_i+1}} \\ &= \chi^{\sigma} \sum_{a_1=0}^{\infty} ... \sum_{a_\sigma=0}^{\infty} \frac{1}{s^{a_1+a_2+...+a_\sigma+\sigma}} \prod_{i=1}^{\sigma} \Gamma\left(\frac{1+c+a_i}{c}\right) (-\chi)^{a_i}. \end{aligned} \tag{4.39}$$

Now taking the inverse Laplace transform of $[\mathcal{F}(s)]^{\sigma}$, we get the PDF of received power, $f_{P_r}(p_r)$, which is

$$f_{P_r}(p_r) = \chi^{\sigma} \sum_{a_1=0}^{\infty} \cdots \sum_{a_\sigma=0}^{\infty} \frac{p_r^{a_1+a_2+\ldots+a_\sigma+\sigma-1}}{(a_1+a_2+\ldots+a_\sigma+\sigma-1)!} \prod_{i=1}^{\sigma} \Gamma\left(\frac{1+c+a_i}{c}\right) (-\chi)^{a_i}. \tag{4.40}$$

Integrating $f_{P_r}(p_r)$ with respect to p_r, we get the CDF, $F_{P_r}(p_r)$ of the received power. The outage probability, $P_o = F_{P_r}(\tau/P_t)$, is thus obtained as in (4.36).

□

After obtaining the outage probability of a node, we calculate the state transition probabilities of $\mathbf{H}$ using (4.8) with the help of the outage probabilities, P_o, calculated from (4.36). The PF eigenvalue, ρ, and the corresponding maximum left eigenvector, $\mathbf{v}$, is calculated such that

$$\mathbf{vH} = \rho\mathbf{v}. \tag{4.41}$$

This enables us to find the unconditional probability for the system to be in state s at hop instant m, which is given as

$$\mathbb{P}\{\mathcal{B}(m) = s\} = \rho^m \mathbf{v}_s, \quad s \in \mathbf{S}, \quad m > 0. \tag{4.42}$$

4.2.4 Special Case: Alternate way to derive the distribution of power for SISO Networks

In this section, we describe an alternate technique for the outage analysis of SISO network in Fig. 4.1. In Theorem 1, we found the approximate distribution of the received power at a node in a SISO network. However, if a

multi-hop SISO network is studied, we can evaluate the outage probability more precisely with the help of numerical integration. Since the ratio distribution, $F_R(r)$, is given by the integral in (4.32), we use the exact PDF, $f_\nu(\nu)$ in (4.19) of distance raised to an arbitrary power, α, in place of its Weibull approximation as follows.

$$\begin{aligned}\widetilde{F}_R(r) &= \int_0^\infty F_\mu(r\nu) f_\nu(\nu) d\nu \\ &= 1 - \left[\int_0^{L^\alpha} (e^{-r\nu}) f_{\nu_1}(\nu) d\nu + \int_{L^\alpha}^{(\sqrt{2}L)^\alpha} (e^{-r\nu}) f_{\nu_2}(\nu) d\nu + \right. \\ &\qquad \left. \ldots + \int_{(2L)^\alpha}^{(\sqrt{5}L)^\alpha} (e^{-r\nu}) f_{\nu_4}(\nu) d\nu \right], \end{aligned} \tag{4.43}$$

where $f_{\nu_1}(\nu), ..., f_{\nu_4}(\nu)$ are the individual pieces of the piece-wise function in (4.19). The integral in (4.43) is solved numerically using Gauss-Legendre integration [46] and is given as

(4.44)

$$\begin{aligned}\widetilde{F}_R(r) \approxeq 1 - \left[\frac{L^\alpha}{2} \sum_{j=1}^{m} \xi_j f_{\nu_1} \left(\frac{L^\alpha}{2} \nu_j + \frac{L^\alpha}{2} \right) + \ldots \right. \\ \left. + \frac{(\sqrt{5}L)^\alpha - (2L)^\alpha}{2} \sum_{j=1}^{m} \xi_j f_{\nu_4} \left(\frac{(\sqrt{5}L)^\alpha - (2L)^\alpha}{2} \nu_j + \frac{(2L)^\alpha + (\sqrt{5}L)^\alpha}{2} \right) \right].\end{aligned}$$

The evaluation points, ν_j, are the roots of mth-order Legendre Polynomials and ξ_j are the corresponding weights. We will observe in Chapter 5 that the results produced through this method are slightly more accurate. However, this approach is only applicable on the SISO network and cannot be extended for the MISO network in Fig. 3.1.

Chapter 5

Results and System Performance

In this section, we verify our analytical models and present some useful results pertaining to the performance of networks in Figs. 3.1 and 4.1. We first plot the PDF of the squared Euclidean distance given in (4.10) and compare it with network simulations. In network simulations, two nodes are randomly placed in their respective regions and the Euclidean distance between them is computed over a million iterations to average the results. It can be seen in Fig. 5.1 that the analytical results exactly match the simulation results for all values of region length L, which shows the accuracy of (4.10). The PDF of the squared Euclidean distance is then plotted and compared with the approximated Weibull PDF in (4.26) for different values of L as shown in Fig. 5.2. The computed mean squared error (MSE) between the actual and the approximated distribution is of the order 10^{-5}. It can be noticed that the Weibull distribution with computed moments is a close fit to the squared distance distribution in (4.10).

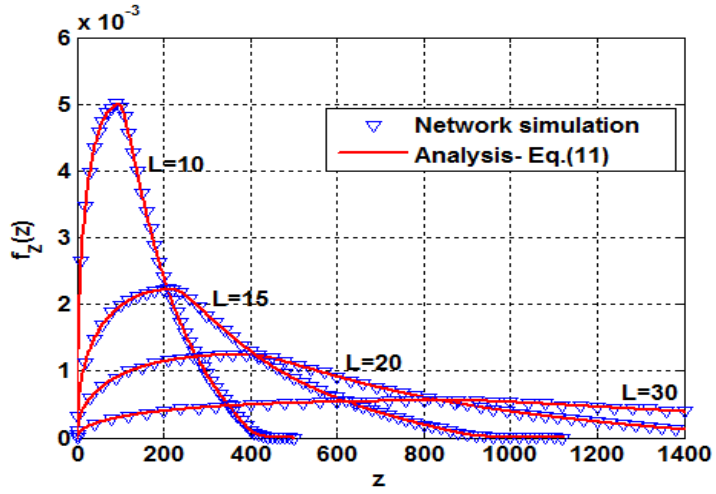

Figure 5.1: PDF of the squared distance using the analytical as well as simulation model, for various region lengths L.

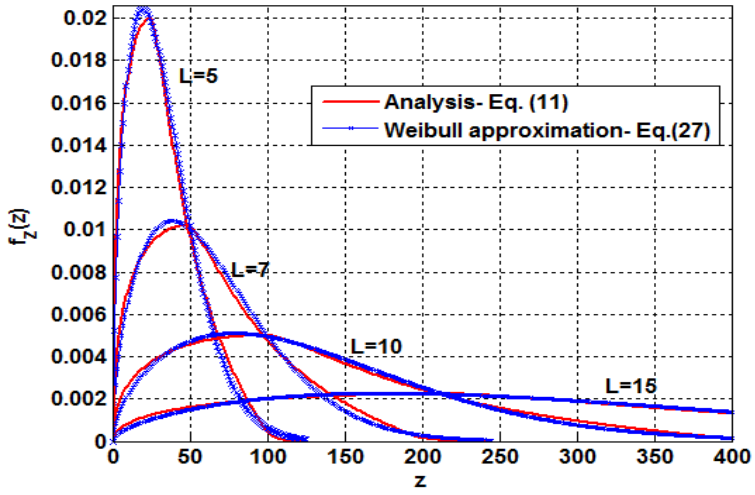

Figure 5.2: Comparison of the analytical PDF of the squared distance with the matched Weibull distribution (shape parameter, $k = 1.5806$, scale parameter, $\lambda = 4L^2/(3\Gamma(1.6327))$ for various region lengths L.

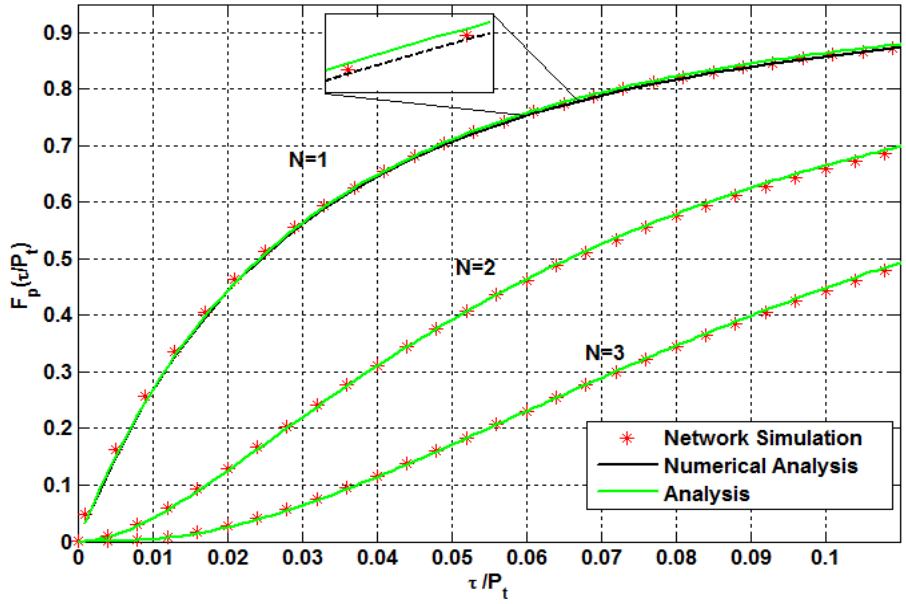

Figure 5.3: Effect of increasing the number of nodes, N, per level on the outage probability. $L = 5, \alpha = 2, P_t = 1$.

Fig. 5.3 validates the expressions for the outage probability derived in Theorem 1 and 2. It can be observed that the network simulation results match with the findings of Theorem 1 and 2. The $N = 2$ and $N = 3$ cases represent the virtual MISO outage probabilities, whereas $N = 1$ represents the SISO case (Fig. 4.1). The additional dashed line in case of $N = 1$ corresponds to the outage probability using Gauss-Legendre numerical integration in (4.44). A zoomed view of the plot for the SISO case and the calculated MSE for various set of parameters shows that numerical integration provides a slightly better approximation to the network simulations as compared to the expression in Theorem 1.

After the verification of outage probabilities, we move on to the Markov chain analysis of the multi-hop strip network. Fig. 5.4 shows the uncon-

ditional state probabilities calculated in (4.42) for different hop counts, m, and compared with the network simulations for $N = 2$. When $N = 2$, each level consists of two nodes placed randomly and there could be two possible transient states of the system; either one node becomes DF (state **1**) or both nodes become DF (state **2**). The figure shows the probability of occurrence of these states at various hops. For simulation purposes, N nodes are generated at random in each level and the first level is assigned a random initial state. To determine the state of a level n, the values for the individual binary indicator functions, $\mathbb{I}_i(n)$, are calculated on the basis of whether the sum of power received from level $(n-1)$ exceeds the decoding threshold, τ, or not. This process is repeated over a million trials to find the state distribution at a certain hop, m. We can see in the network simulation results that initially both states are equally likely with probability $1/2$. However, as the hop count increases, the state probabilities follow the quasi-stationary distribution obtained in (4.5). It can be further noticed that for $N = 2$, the probability of the system to be present in active states **1** or **2** gradually decreases as the number of hops increases and the system will eventually enter the absorbing state **0**, terminating the process of transmissions.

Fig. 5.5 shows the effect of increasing the number of nodes, N, and changing the path loss exponent, α, on the one-hop-success probability, ρ, which is the PF eigenvalue of the sub-stochastic matrix, $\tilde{\mathbf{H}}$. It can be seen that for a particular value of the SNR margin, $\psi = P_t/\tau$, increasing the number of nodes increases the one-hop success probability indicating the increased diversity gain. In the case where $N = 1$, adding another node greatly increases the one-hop success probability. Whereas, when $N = 3$ and

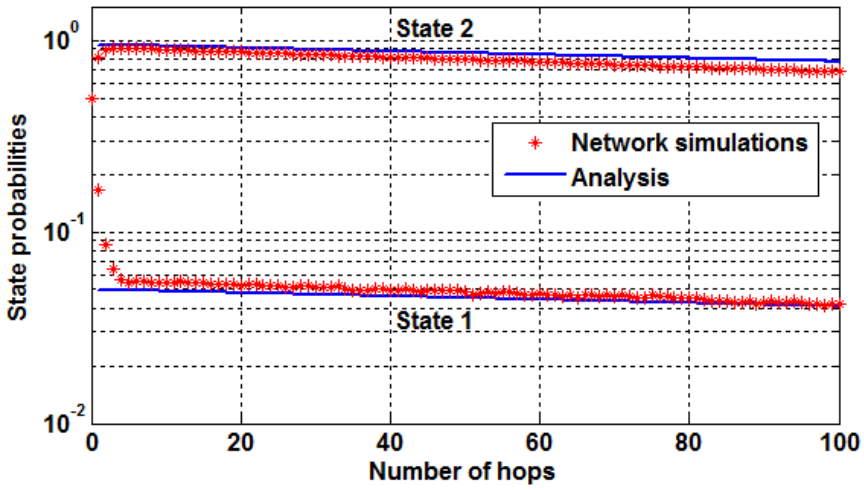

Figure 5.4: Distribution of state probabilities for $N = 2, L = 4, \alpha = 2$ and $P_t = 1$.

a node is added, the rise in the one-hop success probability is not as significant and diminishing returns in the diversity gains are evident. Furthermore, when the path loss exponent is increased from $\alpha = 2$ to $\alpha = 3$, a higher SNR margin is required to get the same one-hop success probability. The curves of one-hop success probability corresponding to $\alpha = 3$ are more flattened.

In case of the actual deployment of the multi-hop strip network, it is important to calculate the coverage range (CR) where the message can successfully reach. The quality of service parameter, η, which is the desired end-to-end success probability, determines the CR. If the message propagates m hops through the strip, the m-hop success probability will be ρ^m. Then η acts as an upper bound to this m-hop success probability, which implies $\rho^m \geq \eta$. As the value of ρ is fixed for a particular set of parameters $(L, \alpha, P_t, \text{etc.})$ and the QoS parameter η is specified, the number of hops, m,

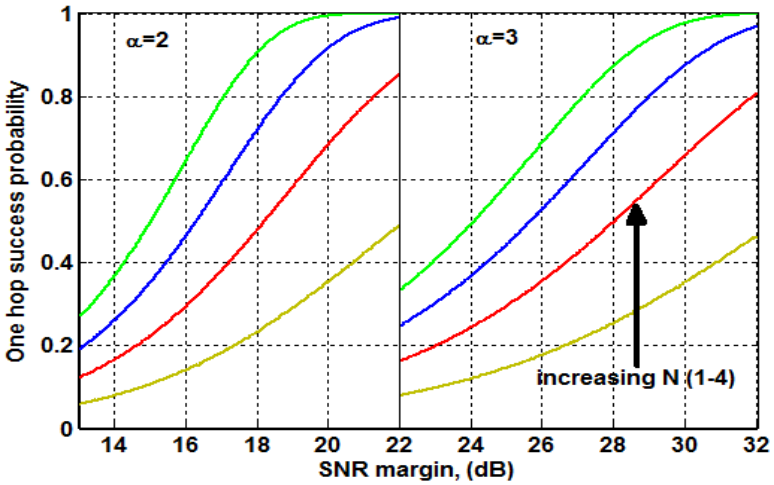

Figure 5.5: Effect of the number of nodes, N, and path loss exponent, α, on one hop success probabilities; $L = 10$.

the message will traverse can be calculated as

$$m \leq \frac{\ln \eta}{\ln \rho}. \tag{5.1}$$

The average CR, therefore, is given as

$$CR = mL. \tag{5.2}$$

Fig. 5.6 shows the contours of CR plotted against the SNR margin, ψ, and region lengths L. It can be observed that for the same transmit power, the message propagates to a larger distance when the width of the network is small. This behavior can be attributed to the fact that path loss plays a significant role in reducing the coverage of a network. As we increase L, we are effectively increasing the signal attenuation because the average distance between a pair of node increases. Another interesting conclusion that can be drawn from this plot is that in order to maintain a particular value of CR,

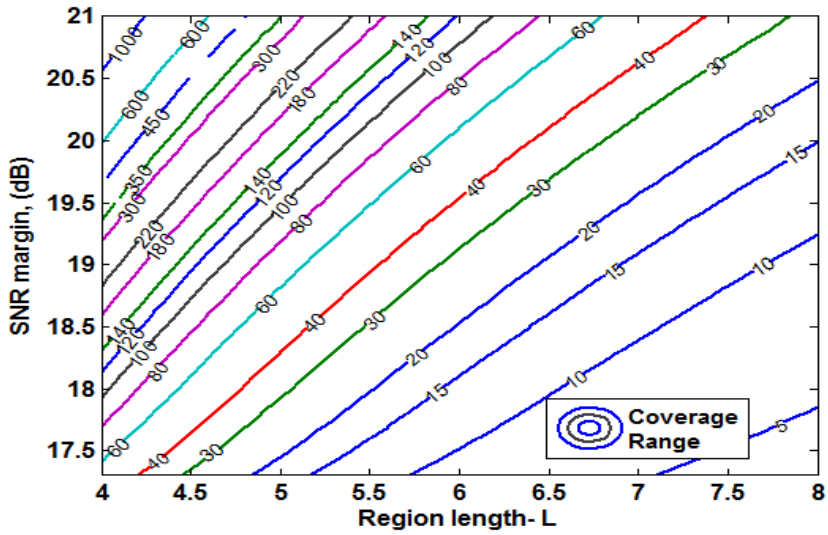

Figure 5.6: Coverage range for various values of region lengths, L and SNR margin $\psi; \alpha = 2, \eta = 0.8, N = 2$.

a network designer may set several different combinations of P_t and L. For power constrained applications, small size networks and low transmit power (or SNR margin) can achieve the desired value of CR. However, for delay constrained applications, larger networks with fewer hops can achieve the same value of CR at the expense of high transmit power.

Chapter 6

Conclusion and Future Work

In this research, we developed a quasi-stationary Markov chain model for the analysis of strip-shaped multi-hop network with fixed non-overlapping square levels in the presence of Rayleigh fading and path loss with an arbitrary exponent. We derived the exact PDF of the Euclidean distance between two nodes in disjoint regions and to make this function analytically tractable, we approximated it with the Weibull PDF. The outage probability of a node is then calculated by deriving the ratio of exponential and Weibull RVs and the sum of the ratio of exponential and Weibull RVs for SISO and MISO networks, respectively. Using outage probabilities, we set up a state transition probability matrix, which enabled us to compute the one-hop success probability and the distribution of active states of the system.

We suggest the following as future directions of this work:

- Rectangular regions- The first step to relax the fixed $L \times L$ regions constraint is to do the analysis all over again with $L \times W$ regions. This will potentially change the mathematical analysis as now the distance

distribution at the very beginning will not be the same. It is yet to explored whether the Euclidean distance will still be Weibull distributed.

- Random number of nodes- Since we kept a constant number of nodes per level, a good addition to this work will be having random number of nodes per level. The number of nodes may be drawn from a Poisson process. The expression for the distribution of power for virtual MISO will change and also, the state transition matrix of the quasi-stationary Markov chain will be a rectangular matrix.

- Removing fixed-boundary constraint- The states of the Markov chain depend on the number nodes present inside an arbitrary window created because of our fixed-boundary constraint. It will be interesting to see how can the fixed-boundary constraint can be removed all together to model pure OLAs.

Bibliography

[1] S. A. Hassan, "Stochastic modeling of cooperative wireless multi-hop networks," 2011.

[2] J. N. Darroch and E. Seneta, "On quasi-stationary distributions in absorbing discrete-time finite markov chains," *Journal of Applied Probability*, vol. 2, no. 1, pp. 88–100, 1965.

[3] A. Sendonaris, E. Erkip, and B. Aazhang, "User cooperation diversity. part ii. implementation aspects and performance analysis," *IEEE Trans. Commun.*, vol. 51, pp. 1939–1948, Nov. 2003.

[4] J. N. Laneman, D. N. Tse, and G. W. Wornell, "Cooperative diversity in wireless networks: Efficient protocols and outage behavior," *IEEE Trans. Inf. Theory*, vol. 50, pp. 3062–3080, Dec. 2004.

[5] S. A. Hassan and M. A. Ingram, "Snr estimation for a non-coherent m-fsk receiver in a slow flat fading environment," in *IEEE Intl. Conf. Communications (ICC)*, pp. 1–5, May.

[6] S. A. Hassan and M. A. Ingram, "Snr estimation for a non-coherent binary frequency shift keying receiver," in *IEEE Global Telecommunications Conference (GLOBECOM)*, pp. 1–5, Nov.-Dec. 2009.

[7] S. A. Hassan and M. A. Ingram, "Snr estimation in a non-coherent bfsk receiver with a carrier frequency offset," *IEEE Transactions on Signal Processing*, vol. 59, pp. 3481–3486, July 2011.

[8] L. Sankaranarayanan, G. Kramer, and N. B. Mandayam, "Cooperative diversity in wireless networks: A geometry-inclusive analysis," in *Proc. Annual ACCCC*, pp. 1598–1607, Sept. 2005.

[9] S. A. Hassan and P. S. Wang, "A dual relay transmission system for wireless communications: Power allocations and channel capacity," in *10th IEEE Intl. Wireless and Microwave Technology Conference (WAMICON)*, pp. 1–4, Apr. 2009.

[10] K. Victor, Y. Wu, and Y. Li, "Error rate performance in ofdm-based cooperative networks," in *Proc. IEEE GLOBECOM*, pp. 3447–3451.

[11] S. A. Hassan, G. Y. Li, P. S. S. Wang, and M. W. Green, "A full rate dual relay cooperative approach for wireless systems," *IEEE Journal on Communications and Networks (JCN)*, vol. 12, pp. 442–448, Oct. 2010.

[12] M. Bacha and S. A. Hassan, "Distributed versus cluster-based cooperative linear networks: A range extension study in suzuki fading environments," in *accepted for publication at IEEE Personal Indoor and Mobile Radio Communications (PIMRC)*, Sept. 2013.

[13] S. A. Hassan, "Range extension using optimal node deployment in linear multi-hop cooperative networks," in *IEEE Radio and Wireless Symposium (RWS)*, pp. 364–366, Jan.

[14] A. Bletsas, A. Khisti, D. P. Reed, and A. Lippman, "A simple cooperative diversity method based on network path selection," *Selected Areas in Communications, IEEE J. Sel. Areas Commun.*, vol. 24, pp. 659–672, Mar. 2006.

[15] A. Bletsas, H. Shin, and M. Z. Win, "Cooperative communications with outage-optimal opportunistic relaying," *IEEE Trans. Wireless Commun.*, vol. 6, pp. 3450–3460, Sept. 2007.

[16] R. Tannious and A. Nosratinia, "Spectrally-efficient relay selection with limited feedback," *IEEE J. Sel Areas Commun.*, vol. 26, pp. 1419–1428, Oct. 2008.

[17] A. Scaglione and Y.-W. Hong, "Opportunistic large arrays: Cooperative transmission in wireless multihop ad hoc networks to reach far distances," *IEEE Trans. Signal Processing,*, vol. 51, no. 8, pp. 2082–2092, 2003.

[18] Y.-W. Hong and A. Scaglione, "Energy-efficient broadcasting with cooperative transmissions in wireless sensor networks," *IEEE Trans. Wireless Commun.*, vol. 5, pp. 2844–2855, Oct. 2006.

[19] P. Herhold, E. Zimmermann, and G. Fettweis, "Cooperative multi-hop transmission in wireless networks," *Computer Networks*, vol. 49, no. 3, pp. 299–324, 2005.

[20] L. V. Thanayankizil, A. Kailas, and M. A. Ingram, "Routing protocols for wireless sensor networks that have an opportunistic large array (ola) physical layer.," *Ad Hoc & Sensor Wireless Networks*, vol. 8, no. 1-2, pp. 79–117, 2009.

[21] B. Sirkeci-Mergen and A. Scaglione, "On the power efficiency of cooperative broadcast in dense wireless networks," *IEEE J. Sel. Areas Commun.*, vol. 25, pp. 497–507, Feb 2007.

[22] B. Sirkeci-Mergen, A. Scaglione, and G. Mergen, "Asymptotic analysis of multistage cooperative broadcast in wireless networks," *IEEE Trans. Inf. Theory*, vol. 52, pp. 2531–2550, June 2006.

[23] L. V. Thanayankizil, A. Kailas, and M. A. Ingram, "Two energy-saving schemes for cooperative transmission with opportunistic large arrays," in *Proc. 50th Annual IEEE Global Telecommunications Conference (GLOBECOM)*, pp. 1038–1042, 2007.

[24] L. V. Thanayankizil and A. Kailas, "Energy-efficient strategies for cooperative communications in wireless sensor networks," in *Proc. 1st IEEE International Conference on Sensor Technologies and Applications (SENSORCOMM)*, pp. 541–546, Oct. 2007.

[25] A. Kailas, L. Thanayankizil, and M. A. Ingram, "Power allocation and self-scheduling for cooperative transmission using opportunistic large arrays," in *Proc. 26th Annual IEEE Military Communications Conference (MILCOM)*, pp. 1–7, Oct. 2007.

[26] A. Kailas, L. Thanayankizil, and M. A. Ingram, "A simple cooperative transmission protocol for energy-efficient broadcasting over multi-hop wireless networks," *Journal of Communications and Networks (Special Issue on Wireless Cooperative Transmission and Its Applications)*, vol. 10, pp. 213–220, Apr. 2008.

[27] A. Kailas and M. A. Ingram, "Alternating cooperative transmission for energy-efficient broadcasting," in *Proc. 51st Annual IEEE Global Telecommunications Conference (GLOBECOM)*, pp. 1–5, Dec. 2008.

[28] A. Kailas and M. Ingram, "Alternating opportunistic large arrays in broadcasting for network lifetime extension," *IEEE Trans. Wireless Commun.*, vol. 8, pp. 2831–2835, June 2009.

[29] A. Kailas and M. A. Ingram, "Investigating multiple alternating cooperative broadcasts to enhance network longevity," in *Proc. IEEE International Conference on Communications (ICC)*, pp. 1–5, June 2009.

[30] S. A. Hassan, "Performance analysis of cooperative multi-hop strip networks," *Wireless Personal Communications*, pp. 1–10, June 2013.

[31] S. A. Hassan, P. Wang, M. Green, and G. Y. Li, "Equalization for symmetric cooperative relay scheme for wireless communications," in *11th IEEERadio and Wireless Symposium (RWS)*, pp. 203–206, Jan.

[32] B. Sirkeci-Mersen and A. Scaglione, "A continuum approach to dense wireless networks with cooperation," in *Proc. IEEE INFOCOM*, vol. 4, pp. 2755–2763, IEEE, Mar. 2005.

[33] S. A. Hassan and M. A. Ingram, "A quasi-stationary markov chain model of a cooperative multi-hop linear network," *IEEE Trans. Wireless Commun.*, vol. 10, pp. 2306–2315, July 2011.

[34] S. A. Hassan and M. A. Ingram, "On the modeling of randomized distributed cooperation for linear multi-hop networks," in *Proc. IEEE Intl. Conf. Commun. (ICC)*, pp. 366–370, IEEE, 2012.

[35] S. A. Hassan and M. A. Ingram, "The benefit of co-locating groups of nodes in cooperative line networks," *IEEE Communications Letters*, vol. 16, pp. 234–237, Feb.

[36] L. V. Thanayankizil and M. A. Ingram, "Opportunistic large array concentric routing algorithm (OLACRA) over wireless fading channels," in *IEEE Globecom Workshops*, pp. 1–5, 2007.

[37] Y. J. Chang, H. Jung, and M. A. Ingram, "Demonstration of an OLA-based cooperative routing protocol in an indoor environment," in *Proc. 17th European Wireless Conf.*, pp. 1–8, VDE, Apr. 2011.

[38] D. Moltchanov, "Survey paper: Distance distributions in random networks," *Ad Hoc Netw.*, vol. 10, pp. 1146–1166, Aug. 2012.

[39] S. Srinivasa and M. Haenggi, "Distance distributions in finite uniformly random networks: Theory and applications," *IEEE Trans. Veh. Technol.*, vol. 59, no. 2, pp. 940–949, 2010.

[40] A. Kostin, "Probability distribution of distance between pairs of nearest stations in wireless network," *Electronics Letters*, vol. 46, no. 18, pp. 1299–1300, 2010.

[41] E. Senta, *Non-Negative Matrices and Markov Chains, 2nd edition.* Springer, 2006.

[42] S. A. Klugman, H. H. Panjer, G. E. Willmot, and G. G. Venter, *Loss Models: From Data to Decisions*, vol. 2. Wiley New York, 1998.

[43] S. M. Kay, *Fundamentals of Statistical Signal Processing, volume I: Estimation Theory (v. 1).* Prentice Hall, 1998.

[44] S. Nadarajah and S. Kotz, "On the product and ratio of Gamma and Weibull random variables," *Econometric Theory*, vol. 22, no. 02, pp. 338–344, 2006.

[45] A. Prudnikov, Y. A. Brychkov, and O. Marichev, *Integrals and Series: Special Functions, vol. II.* Gordon and Breach Science Publishers, 1986.

[46] P. J. Davis and P. Rabinowitz, *Methods of Numerical Integration.* Courier Dover Publications, 2007.